Transactions of the Materials Research Society of Japan. Vol. 20
© 1996 MRS-J. All rights reserved.

Infra-red Absorption in Hydrogenated Amorphous Carbon (a-C:H) Films

Kaoru Kitakizaki[a], Yasuhiko Fujita[b]

[a]Reseach & Development Headquarters, Meidensha Corporation
1-17 Ohsaki 2-chome, Shinagawa-ku, Tokyo 141 Japan

[b]Department of Electronic Systems Engineering, Tokyo Metropolitan Institute of Technology
6-6, Asahigaoka, Hino, Tokyo 191 Japan

Cathodic a-C:H films with photoconductive nature were prepared from a gas mixture of CH_4 and H_2 by rf-PECVD with a third electrode inserted between the anode and cathode electrodes. The hydrogen bonding configuration CHn, the deconvolution of IR absorption spectra over the range of 2700 ~ 3200 cm^{-1} and optical gap Eopt have been investigated for the cathodic and anodic films. The bonding ratio sp^3/sp^2 of the cathodic films are small and constant at annealing temperatures of TA = 250-500 °C, compared with those of anodic films. For the cathodic films Eopt is ~1.25 eV and the anodic films Eopt ~1.75 eV, and these values decrease above TA ~ 600 °C. This result could be explained by considering the sp^3/sp^2 ratio for the carbon atoms and the amount of CHn in the cathodic and anodic a-C:H films.

1. Introduction

It is well known that hydrogenated amorphous carbon (a-C:H) films have a potential as the materials of modern electronic devices such as light emitting diodes and magnetic recording devices etc., in addition to other practical applications using its superior mechanical properties and chemical inertness. In this respect, many studies have been done for a-C:H prepared by several kinds of technical methods with respect to the electrical and structural properties like hydrogen bonding configurations based on infra-red absorption measurements[1,2].

However, it is unsatisfactory for the preparation of a-C:H with the required opto-device performance because the electrical and optical properties of a-C:H are not fully understood. For instance, there are only few reports that the photocurrent was observed in a-C:H, playing the important role in the photoelectronic behavior[3,4].

The purpose of the present study is to clarify the bonding configurations of hydrogen (i.e., CH, CH_2 and CH_3) and the deconvolution of IR absorption spectra over the range of 2700-3200 cm^{-1} for cathodic a-C:H films (showing the good photoconductive nature) and anodic ones, which were prepared from CH_4 and H_2 mixture by rf plasma-enhanced chemical vapor deposition (PECVD) with a negatively biased third electrode inserted between the cathode and anode electrodes. This kind of study is made for the first time in our knowledge. Furthermore, we investigated the annealing characteristics over the temperature range from 250 to 750 °C of the cathodic a-C:H films on the deconvolution of IR absorption spectra, hydrogen bonding configurations, and optical gap on the basis of FT-IR spectra and optical absorption coefficient measurements, and compared with the corresponding results of the anodic a-C:H films.

2. Experimental details

Cathodic films of a-C:H were deposited onto the quartz and silicon substrates set on the cathode electrode in article rf PECVD chamber. The diameter of the cathode and anode electrodes was 10 cm and the distance between them was 2.6 cm. In order to obtain the cathodic films with the photoconductive nature, a third mesh electrode was inserted between the two electrodes. Gas mixture of pure methane and hydrogen was introduced into the chamber. The fraction of H_2 gases, $H_2/(CH_4+H_2)$ was kept at 60 % and total gas pressure was maintained at 0.03 Torr with a gas flow rate of 20 ccm. The rf power density was maintained at 0.64 W/cm^2, and the bias voltage was to be -0.48~-0.45 kV. During the deposition run, the current with several hundred μA was flowed into the third electrode biased at -20 V. The substrate temperature of the cathodic films was maintained at about 150 °C during the deposition run.

Anodic films of a-C:H were also deposited on the quartz and silicon substrates set on the anode electrode, and the deposition condition was the same as those of the cathodic films except for removing the third electrode and the substrate temperature 50 °C. The deposition rate was 3.1 Å/s and 1.3 Å/s for the cathodic and anodic films, respectively, and the thickness of both films was kept at about 1 μm.

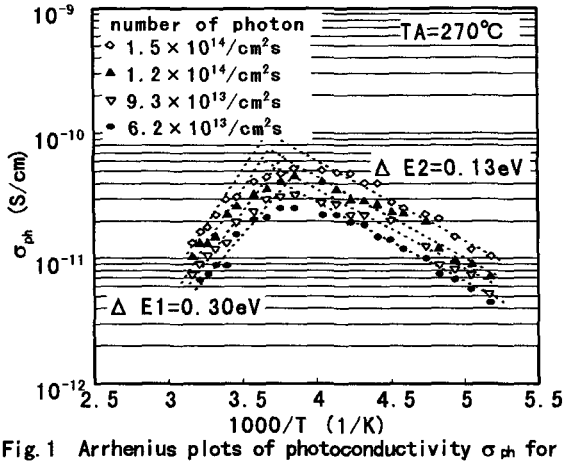

Fig. 1 Arrhenius plots of photoconductivity σ_{ph} for the cathodic films annealed at 270 °C for 1 hour.

After all the films were prepared, they were annealed at temperature TA for 1 hour in vacuum less than 5×10^{-6} Torr. TA adopted here was 250, 350, 500, 600, 700 and 750 °C. We investigated the C-H bonding configuration, the ratio of sp^3 to sp^2 bonding, and optical band gap (Eopt) in the cathodic and anodic (a-C:H) films based on FT-IR and optical absorption measurements as a function of annealing temperature TA.

3. Results and discussion

In order to show the photoconductive nature, Arrhenius plots of photoconductivity σ_{ph} are presented in Fig. 1 for the cathodic a-C:H films annealed at 270 °C for 1 hour. It is seen that there are peaks of σ_{ph} similar to those of the previous reports on amorphous silicon and chalcogenide semiconductors[5,6]. Fig. 1 suggests that the photo-carriers are dominated by the thermally activated photoconduction associated with disorder like the band tail and the gap states. The details of these photoconductive nature will be reported in a forthcoming paper.

Fig. 2 shows the carbon-hydrogen (C-H) stretching absorption spectra over the range of 2700-3200 cm^{-1} for the as-deposited cathodic films (with silicon substrate) and those annealed at TA = 600, 700, and 750 °C. From the absorption spectra shown in Fig. 2, we determined the structure of C-H bond and the ratio of carbon bond tetrahedral (sp^3) to graphitic (sp^2), sp^3/sp^2, assuming the absorption modes of CH, CH_2, and CH_3 with Gaussian functions irrespective of each annealing temperature. Comparing these spectra with those of a-C:H films reported previously, we identify the main peaks as follows[7-11]: The peaks of 3040 cm^{-1}, 3000 cm^{-1}, and 2960 cm^{-1} correspond to a sp^2CH aromatic stretching mode, a sp^2CH olefinic stretching mode and a sp^3CH_3 asymmetric stretching mode, respectively. Furthermore,

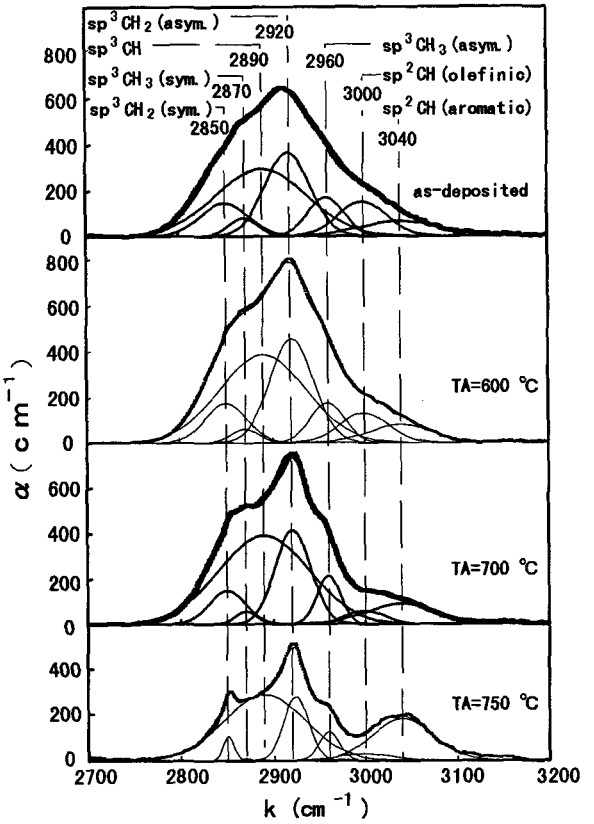

Fig. 2 The C-H stretching absorption spectra for the as-deposited cathodic films and those annealed at TA = 600, 700 and 750 °C.

the peaks at 2920 cm^{-1}, 2890 cm^{-1}, 2870 cm^{-1}, 2850 cm^{-1} correspond to the sp^3CH_2 asymmetric stretching mode, the sp^3CH stretching mode, the sp^3CH_3 symmetric and the sp^3CH_2 symmetric stretching mode, respectively. Dischler et al.[12] have reported the sp^3CH stretching mode appeared at 2920 cm^{-1}, whereas Shimada et al. reported the sp^3CH appeared at 2890 cm^{-1} [13]. We used the sp^3CH stretching mode at 2890 cm^{-1}, which naturally coincides with the present results. On the other hand, the stretching absorption spectra for the cathodic films annealed at TA = 250, 350, and 500 °C were almost the same as those of as-deposited cathodic films shown in Fig. 2. In Fig. 2 one can find the reduction of peaks at 2960 cm^{-1} (sp^3CH_3 asymmetric stretching mode), 2870 cm^{-1} (sp^3CH_3 symmetric stretching mode) and 3000 cm^{-1} (sp^2CH olefinic stretching mode) as the annealing temperature increases. In contrast, the peak of the sp^2CH aromatic stretching mode at 3040 cm^{-1} increases. It is also found from Fig. 2 that the absorption profiles of the cathodic films show the widely spread ones. This suggests that a large amount of disorder exists in the cathodic films compared with the crystalline carbon.

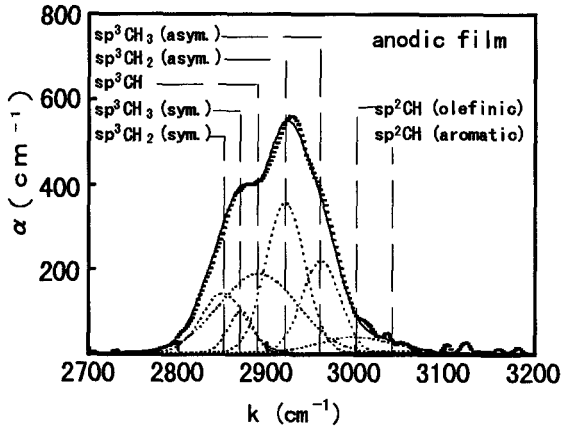

Fig. 3 The C-H stretching absorption spectra and the deconvolution into subbands of the as-deposited anodic films.

Fig. 3 shows the C-H stretching absorption spectra for the as-deposited anodic films taken over the range of 2700-3200 cm^{-1}. Here, the spreading of this spectrum is less than that of the as-deposited cathodic films shown in Fig. 2. This suggests that the disorder in the as-deposited anodic films also less compared with that in the cathodic films. In Fig. 3, the deconvolution of the absorption spectra into some subbands is also presented.

Fig. 4 shows the ratio of sp^3 to sp^2 bonds for the cathodic and anodic films plotted against the annealing temperature TA. One can find from Fig. 4 that the values of sp^3/sp^2 for the anodic films are larger than those of the cathodic ones. On the other hand, the dynamic hardness of the anodic films was to be 160 kgf/mm^2, which is smaller than 750 kgf/mm^2 of the cathodic ones. This means that a large amount of C-H terminal exists in the anodic films, so that their films are of polymer-like. In contrast, the cathodic films contain a less sp^3/sp^2 ratio , a more CH and a less CH_3 bonds in the sp^3 structure compared with those in the anodic

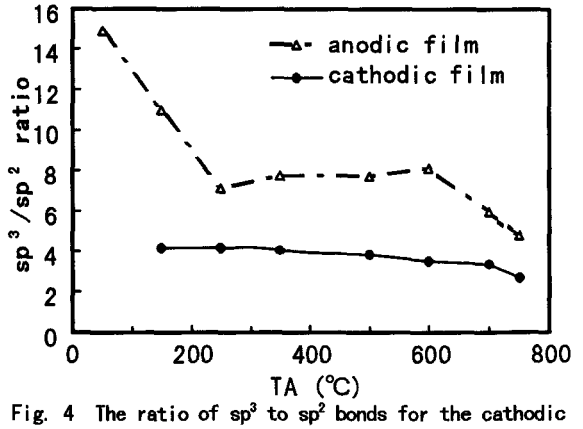

Fig. 4 The ratio of sp^3 to sp^2 bonds for the cathodic and anodic films plotted against the annealing temperature TA.

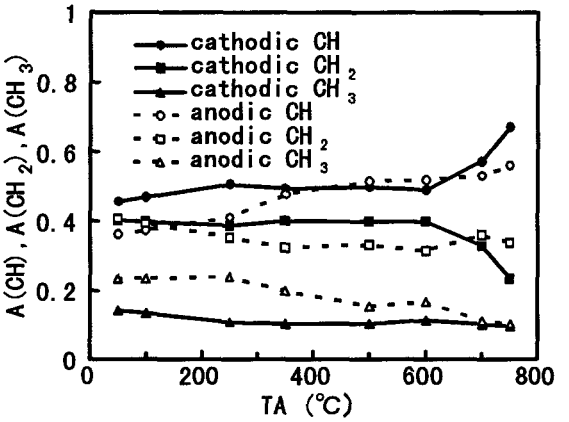

Fig. 5 The ratio CHn/Σ CHn for the cathodic and anodic films plotted against the annealing temperature TA.

films, as will be mentioned later. From this, the cathodic films with the more C-H bonds are expected to contain the more C-C bonds, which contribute to form a three-dimensional network, because a-C:H is considered to be constructed by the tetrahedrally coordinated carbon. Tachibana et al. reported that methane plasma mainly comprises of radicals, positive ions and electrons, and negative ions are very scarce[14]. In our experiments, the negative bias (-0.48 ~ -0.45 kV) applied to the cathode electrode gives a kinetic energy to the positive ions and radicals around the cathode electrode. Then, the weakly bonded high-order CHn such as CH_2 and CH_3 will be etched preferentially by the bombardment of the positive ions and radicals. Consequently, the ratio of C-C (strongly bonded) to C-H bonding is increased and the dynamic hardness is raised for the cathodic films. In our experimental conditions, the deposition rate of the cathodic films showed a higher value (3.1 Å/s) than that of the anodic films (1.3 Å/s). The value of 3.1 Å/s is explained as follows: the positive ions enhanced by the methane plasma potential are largely accelerated toward the negatively biased cathode electrode. The radicals are accumulated softly on the anode electrode because of the very less negative ions, and it gives the small deposition rate for the anodic films. For both anodic and cathodic films, it is noted that sp^2 structure, which is more stable thermodynamically, increases as TA increases.

In Fig. 5 are shown the analyzed results of the amount of sp^3CH_3, sp^3CH_2 and sp^3CH for the cathodic and anodic films in order to examine the C-H bonding structure. The cathodic film has less sp^3CH_3 and more sp^3CH than those of anodic film. It is generally expected that the CH_3 bonds disturb the creation of three dimensional cross-linking of carbon skeleton, and thus form three terminals of CH_3. One can also expected that a number of CH bonds decrease the terminals of CHn

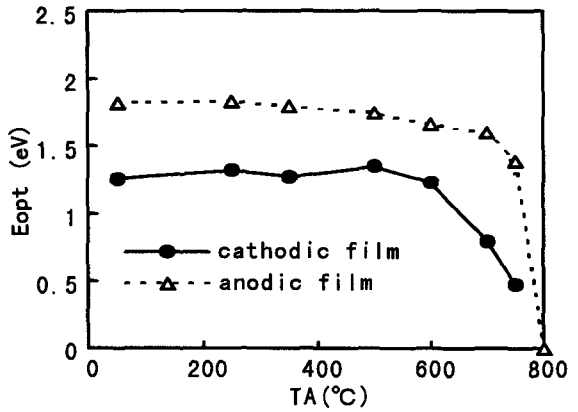

Fig. 6 Eopt of cathodic and anodic films plotted against the annealing temperature TA.

and contribute to creating the three dimensional structure with C-C bonds. Therefore, in the cathodic films, the C-H bonds are large and then CH_3 bonds small in quantity, as shown in Fig. 5. From this, we understand that the values of sp^3/sp^2 of the cathodic films are small and constant over the range of TA investigated, so that the cathodic films show mechanically hard nature. These experimental results are almost consistent with those of the previous reports by other workers, with respect to the FT-IR absorption profile and the sp^3/sp^2, except for no data of the ratio CHn/ΣCHn, as a function of annealing temperature.

Finally, we present experimental results on optical gap (Eopt) and give short discussion on them. The values of Eopt were determined from Tauc plots. They are shown for the cathodic and anodic films with quartz substrate in Fig. 6 as a function of annealing temperature TA. The value of Eopt of the cathodic film remain almost constant at 1.25 eV up to 500 °C and then decrease rapidly above TA = 600 °C. It is pointed out that the value of Eopt = 1.25 eV up to TA = 500 °C of the cathodic films is almost coincident with the values of Eopt = 1.1-1.26 eV of a-C:H annealed at 300 °C for 1 hour, reported by Dixit et al.. On the other hand, the values of Eopt of the anodic film are larger than those of the cathodic film, which decrease rapidly at TA = 700 °C. In this respect, it is known that the optical gap in a-C:H is dominated by the value of sp^3/sp^2 [15]. Surely, it was confirmed that the magnitude of Eopt for the cathodic and anodic films shown in Fig. 6 corresponds approximately to those of sp^3/sp^2, as mentioned above.

4. Conclusion

Cathodic a-C:H films with photoconductive nature were prepared from a gas mixture of CH_4 and H_2 by PECVD with a third electrode inserted between the anode and cathode electrodes. We investigated the hydrogen bonding configuration CHn, the deconvolution of IR absorption spectra over the range of 2700-3200 cm^{-1} and the optical gap Eopt for the cathodic and anodic specimens. It was found that the bonding ratio, sp^3/sp^2, of the cathodic films are small and constant at annealing temperatures of TA = 250-750 °C, compared with those of the anodic films. We have also obtained the results on Eopt as follows. For the cathodic films Eopt ~ 1.25 eV and the anodic films Eopt ~ 1.75 eV, and these values decreased rapidly above TA ~ 600 °C. This result could be explained by considering the ratio sp^3/sp^2 and the amount of CHn in the cathodic and anodic a-C:H films.

Reference

1. Dischler, in Amorphous Hydrogenated carbon Films, edited by P. Koidl and P. Oelhafen (Les Editions de Physique, Paris,) P. 189 (1987)
2. C. De Martino, F. Demichelis and A. Tagliaferro, Diamond Relat. Mater., 4, 1210 (1995)
3. G.A.J. Amaratunga, V.S. Veerasamy, W.I. Milne, C.A. Davis, S.R.P. Silva and H.S. MacKenzie, Appl. Phys. Lett. 63 (3) 370 (1993)
4. P.N. Dixit, Sushil Kumar, D. Sarangi and R. Bhattacharyya, Solid State Commun. 90 (7) 421 (1994)
5. W.E. Spear, R.J. Loveland and A. Al-Sharbaty, J. Non-Crystalline Solids, 15, 410 (1974)
6. T. C. Arnoldussen, R.H. Bube, E.A. Fagen and S. Holmberg, J. Appl. Phys. 43, 1798 (1972)
7. D.R. McKenzie, R.C. McPhedran, N. Savvides, L.C. Botten, Phil. Mag. B, 48, 341 (1983)
8. B. Dischler, A. Bubenzer, P. Koidl, Appl. Phys. Lett., 42, 636 (1983)
9. B. Dischler, A. Bubenzer, P. Koidl, Solid St. Commun., 48, 105 (1983)
10. B. Dischler, E. Bayer, J. Appl. Phys. 68, 1237 (1990)
11. A. Ishii, Y. Sakaguchi, S. Minomo, M. Taniguchi, M. Sugiyo and T. Kobayashi, Jpn. J. Phy. 32, L802 (1993)
12. B. Dischler, A. Bubenzer, P. Koidl, Solid State Commun. 48, 105 (1983)
13. Y. Shimada, N. Matukura and Y. Machi, J. Appl. Phys. 71, 4019 (1992)
14. K. Tachibana, M. Nishida, H. Harima and Y. Urano, J. Phys. D: Appl. Phys., 17, 1727 (1984)
15. S. Kaplan, F. Jansen and M. Machonikin, Appl. Phys. Lett. 47, 750 (1985)